Identification of a VEGFR-3 binding peptide TMVP1 for enhancing drug delivery efficiency and therapeutic efficacy against tumor lymphangiogensis

Liangsheng Fan
Huazhong University of Science and Technology
Teng Cheng
Huazhong University of Science and Technology
Fei Li
Huazhong University of Science and Technology
Zhenzhong Zhang
Huazhong University of Science and Technology
Qingjian Dong
Huazhong University of Science and Technology
Yuan Yuan
Huazhong University of Science and Technology
Xi Chen
Huazhong University of Science and Technology
Ying Zhou
Huazhong University of Science and Technology
Xiaohua Zhu
Huazhong University of Science and Technology
Ding Ma
Huazhong University of Science and Technology
Ling Xi
Huazhong University of Science and Technology
Danfeng Luo
Huazhong University of Science and Technology
Xiangyi Ma (xiangyi_ma@126.com)
Huazhong University of Science and Technology

Research Article

Keywords: TMVP1, VEGFR-3, targeted therapy, tumor lymphatic metastasis, KLA

Posted Date: April 20th, 2022

DOI: https://doi.org/10.21203/rs.3.rs-1517169/v1

Abstract

VEGFR-3 plays an indispensable role in lymphangiogenesis. Previous findings suggest that blocking the VEGFR-3 signaling pathway can inhibit lymph node metastasis effectively, thus reduce the incidence of distant metastasis. The development of new VEGFR-3 targeting drugs for early detection and effective treatments is, therefore, urgently requied. Here, in vitro biopanning of a phage-displayed peptide library was used to identify specific peptides binding to the extracellular domain of VEGFR-3. We obtained a novel VEGFR-3 targeting peptide TMVP1 (LARGR), our combined immunofluorescence and radiopharmaceutical studies revealed that FITC-TMVP1 and ^{99m}Tc-labeled TMVP1 specifically accumulated in VEGFR-3 positive lymphatic vessels of tumors after i.v administration in tumor xenograft models in vivo. The accumulation of the TMVP1 in lymphatic vessels was specific, because this accumulation can be significantly reduced by blocking experiments. To enhance the therapeutic efficacy of anticancer drugs, we fused TMVP1 to a proapoptotic peptide $_{D}$(KLAKLAK)^2, the fusion peptide strongly inhibited tumor lymphangiogenesis in vitro and in vivo, and specifically suppressed lung metastasis in a 4T1 breast cancer xenograft model. Our results suggest that TMVP1 is a promising therapeutic strategy for the development of new diagnostic tracers or alternative anticancer agents for tumor lymphangiogenesis and lymphatic metastasis.

Introduction

Most deaths from cancer occur as a result of metastasis. The lymph nodes adjacent to the primary tumor are often the first site of metastases in many cancer types. Detection of lymph node metastasis is of major prognostic significance in many cancers[1]. Lymph node metastasis is an important clinicopathological parameter for cancer prognostication and treatment. The therapeutic importance of lymph node metastasis, especially its role in predicting disease progression and determining future post-operative therapies, underscores the necessity of understanding the process of lymph node metastasis[2].

Tumor lymphangiogenesis contributes to tumor progression at least in part by actively facilitating metastatic dissemination to sentinel lymph nodes through a variety of mechanisms[3]. Lymphangiogenesis starts before the onset of metastasis and is associated with distant metastasis. VEGFR-3 plays an indispensable role in lymphangiogenesis[2, 4–6], and it has been identified as one of the main lymphatic specific markers[2, 7], which are widely expressed in embryonic tissues and adult new lymphatic endothelia cells[4, 8]. In recent years, VEGF-C/VEGFR-3 signaling pathways have been confirmed to play important roles in lymphangiogenesis and tumor cell mobility, invasion and metastasis. It has been shown that the blockade of VEGF-C/D–mediated signaling can suppress tumor lymphangiogenesis and lymph node metastases in mice[9, 10]. Inhibition of lymphangiogenesis with a soluble form of VEGFR-3 or monoclonal anti-bodies that block receptor activation can reduce lymphatic metastases by 50%-70% in preclinical models[11]. These findings suggest that blocking the VEGFR-3 signaling pathway can inhibit lymph node metastasis effectively, and thus reduce the incidence of distant metastasis. Therefore

VEGFR-3 blockade is expected to become an effective means of reducing lymph node metastasis by blocking the VEGF-C/VEGFR-3 signaling pathways in cancer therapy[12].

However, antibodies may not reach their molecular targets in sufficient amounts and uniformly to be completely efficacious under conditions of insufficient number of blood vessels, erratic blood flow, and high intratumoral pressure[13]. Short peptides are ideal molecules for targeting tumor cells[14]. Peptide-based therapy has been applied in various diseases, such as allergic diseases, infectious diseases, autoimmune diseases, fibrosis, and asthma. There are several advantages of peptides, such as easy availability and convenient purification and storage[15]. Peptide-based therapies have been tested in both in vitro and in vivo experimental models, and some have presented promising outcomes[14, 15].

On this basis, we used the bacterial peptide display system, FliTrx, to identify a new peptide that binds to the extracellular domain of VEGFR-3. In vitro screening of the FliTrx library with the extracellular domain of VEGFR-3 derived a 5-amino acid peptide, LARGR (termed TMVP1). We carefully assessed the accuracy and specificity of TMVP1 binding to VEGFR-3 in vitro and in vivo, and evaluated the targeting effects and the inhibitory effects of the peptide TMVP1-KLA, which is TMVP1 fused with a proapoptotic peptide $_{D}$(KLAKLAK)^{2}, on lymphangiogenesis in vitro and in vivo[16, 17].

Materials And Methods

Peptide library screening.

A random 12-mer cyclic peptide display library, the FliTrx Random Peptide Display Library (Catalog no. K1125-01, Invitrogen, USA), was used to identify specific peptides binding to the extracellular domain of VEGFR-3. The FliTrx clones targeting recombinant human VEGFR3/Flt-4 (Catalog no.349-F4, R□D systems, USA) were isolated from the FliTrx library by combined *in vitro* screening according to the manufacturer's protocol. For each round, 1 × 10^{8} FliTrx cells were added to a culture dish with the recombinant human IgG for negative selection and then incubated for 1 h with recombinant Human VEGF R3/Flt4 protein for positive selection. After four rounds, 100 individual FliTrx clones were selected, and their peptide-encoding inserts were sequenced and analyzed for potential repetitive peptide motifs. Quantification of binding selectivity was determined by counting the bacterial clones.

Cell lines, reagents and mice. Cell lines, reagents, and mice. Primary human lymphatic endothelial cells (LECs) (Cat2500, ScienCell Research Laboratories, San Diego CA, USA) were cultured in endothelial cell medium. Human umbilical vein endothelial cells (HUVEC), HEK-293 human embryonic kidney cells, the human breast cancer cell lines MDA-MB-231„ and SiHa, the murine breast cancer cell line 4T1 and the *melanoma* cell line B16 were obtained from the American Type Culture Collection. All cell lines were maintained in complete RPMI 1640 or DMEM containing 10% fetal bovine serum. BALB/C mice and Balb/c-nude mice were purchased from the Institute of Laboratory Animal Science, of the Chinese Academy of Medical Sciences. (Beijing, China). Construction of mouse models, breeding, and staging were performed using standard methods.

Peptide design and synthesis. The TMVP1 peptide (LARGR), was designed with the general structure GCGXXXXXGC (XXXXX = variable residue, C = cysteine, and G = glycine), which is flanked by two cysteine residues to allow for disulfide linkage and loop formation[18]. Glycine residues provide a spacer function, permitting the physical formation of a loop structure. FITC was coupled to the peptides via an additional glycine at the NH2 terminus. We fused the peptide TMTP1 to an antimicrobial peptide, $_D$(KLAKLAK)^2, and termed the resulting peptide TMVP1-KLA. LARGR, RGLARGRIGFVM, FITC-TMVP1, HYNIC-TMVP1 and TMVP1-$_D$(KLAKLAK)^2 were synthesized by the WuXi AppTec (Shanghai) company with a purity of >95 %,as analyzed by reversed-phase high-performance liquid chromatography (RP-HPLC) and characterized by electrospray mass spectrometry (MS). HYNIC-TMVP1 was labeled with ^{99m}Tc using a previously described protocol[19, 20].

Evaluation of peptide-protein interaction by SPR and the docking method

Modeller software was used to produce homology models of VEGFR-3. The overall architecture of the extracellular VEGFR-3 (D1-D7) was similar to that of previously reported VEGFR-2[4]; hence, it was built using two templates (PDB_ID: 5T89 and 4BSK). D1-D2 was resolved along with the 4BSK structure, and the residual structure of the extracellular domain of VEGFR-3 was constructed based on the 5T89 template as a model. For local peptide-VEGFR3 docking, the RosettaDock server was used, and the binding pocket for the peptides binding to VEGFR-3 was initially assessed. Meanwhile, thermodynamic analysis of the enthalpy between the peptide and VEGFR-3 D1-7 was also conducted.

The OpenSPR^{TM} instrument (Nicoya Lifesciences Inc., Kitchener, Canada) was used to determine the equilibrium binding constant (KD) of peptides with VEGFR-3. All the steps were performed according to its protocols.

The immunofluorescence test

Ninety-six-well microtiter plates were coated with an appropriate amount **(0.1 μg)** of Recombinant Human VEGF R3/Flt4 protein dissolved in PBS containing 0.05% Tween 20 and incubated overnight at 4°C. Serially diluted FITC-TMVP1 was then incubated for 1 h at room temperature. After thorough washing with PBS containing 0.05% Tween 20, the ability of TMVP1 binding to the target antigen were identified using an immunofluorescence test.

The affinity of FITC-TMVP1 to cells

LECs, HUVEC, and HK293 cells were grown on coverslips overnight. Cells were then incubated with 20 **μ**M FITC-labelled TMVP1 at 37℃ for 60 min, then fixed with 4% paraformaldehyde at room temperature for 10 min. Samples were blocked in 3% BSA (w/v) in PBS for 30 min at room temperature. Cells were then incubated with anti-VEGFR-3 (Ab27278; Abcam, USA) for 60 min at room temperature and washed with PBS three times. Then incubated with cy3-conjugated Goat anti-Rabbit IgG for 30 minutes and followed by nuclear staining with 4,6-diamidino-2-phenylindole (DAPI). A laser scanning confocal microscope was

used to visualize the slides (German Leica, true confocal scanner spectrophotometry, Mannheim, Germany).

Ex vivo fluorescent peptide-binding capacity

The mouse corneal micropocket 4T1 model was used for targeting experiments when the tumors had grown, as previous described. FITC-TMVP1 (210 μg) was injected into the tail vein and allowed to circulate for 1 h. Tumorous organs were excised and immunostained with VEGFR-3 and LYVE-1(ab33682, Abcam, USA), then examined for fluorescence by laser scanning confocal microscopy (Olympus Fluoview FV1000). The biodistribution of FITC-TMVP1 in a 4T1 subcutaneous tumor model, tumor tissues, and normal organs were measured 20 min after injection. The frozen sections were prepared and nuclei were stained with DAPI.

The clinical tissue samples of breast cancer patients were dissected for FITC-TMVP1 binding studies using immunofluorescence assays. Tissues were obtained immediately after surgery, immediately embedded in optimal cutting temperature medium, and then cut into 7 mm-thick frozen sections. The affinity assay of FITC-TMVP1 with the clinical tissue samples of breast cancer tissues was conducted as above.

SPECT imaging and Biodistribution study assay of ^{99m}Tc-HYNIC/EDDA-TMVP1

The imaging study was performed in B16, 4T1 and SiHa tumor-bearing mice using the ^{99m}Tc Thyroid Scan procedure of SPECT, all of which were used for ^{99m}Tc-HYNIC-TMVP1 imaging with or without the excess blocking agent. Each tumor-bearing mouse was injected in the penis vein with ^{99m}Tc-HYNIC-TMVP1 (20 MBq/mouse) in 0.2 mL of saline. The mice were anesthetized using 30–50 μL of 3% pentobarbital sodium salt before SPECT imaging. For the blocking experiment, excess cold HYNIC-TMVP1 (239 nmol dissolved in 0.2 mL of saline) was administered intravenously via the penis vein to three mice 30 min prior to administration of ^{99m}Tc-HYNIC-TMTP1 (20 MBq/mouse). The biodistribution study was conducted in 4T1 tumor models, as described in a previously published article[19, 20].

Three-dimensional bead sprouting assay

The 3D *in vitro* model of angiogenesis was performed as described previously [28-31]. Growth factor-reduced type I collagen (C7661, Sigma-Aldrich) was added to 96-chamber slides with 100 μl ECM and allowed to gel for 30 minutes at 37°C. LECs or macrophages were seeded at densities of 1×10^6 cells/ml in 500 μl of ECM containing 3% FBS. The beads and cells were mixed by gentle swirling, incubated at 37°C for 4-8 hr, and then rotated on an orbital mixer in a 37°C oven to generate endothelial cell-loaded microcarrier beads. Digital pictures were taken using a spot image analysis system, and the areas covered by tube-like structures were measured using NIH Image software at 6 h. The cells were then treated with TMVP1-KLA, recombinant 5 ng/ml rhVEGF-C protein, or5 ng/ml TMVP1-KLA+ rhVEGF-C protein, respectively, for 4-8 hours. The total area covered by the type □ collagen was outlined; the area of the tube-like structures within the type □ collagen was calculated and expressed as a percentage of the

type Ⅳ collagen area. The sprouting assay was performed according to protocols from the literature [32] and quantified with NIH ImagePro Plus 5.0 software.

The inhibitory effect on tumor lymphangiogenesis in vivo

To detect the inhibiton of tumor lymphangiogenesis, the corneal micropocket lymphangiogenesis model was performed as described[21]. The eyes were examined on day 3 or after suture implantation. Four days after tumor transplantation, 150 μM TMVP1-KLA peptide or filter-sterile water was injected intraperitoneally (IP) every other day. Two weeks later treated mice were sacrificed and the corneal tissues were surgically removed for LYVE1 staining. The corneal tumor was removed and frozen. The corneal tumor was removed and frozen. The fixed and paraffinized sections were sectioned for immunohistochemistry for the corresponding blood vessels and lymphatic vessels.

Mouse Experimental Techniques

Four-week-old BALB/c nu/nu mice were obtained from the SLAC Laboratory Animal Co. Ltd (Shanghai, China). MDA-MB-231-derived human breast carcinoma xenografts were established as described above. Five days after tumor transplantation, 50 μM TMVP1-KLA peptide or filter-sterile water was injected intraperitoneally every other day. Tumor growth was measured in three dimensions twice a week using a caliper. Tumor volume was calculated using the formula: length x width^2 x 0.52. Mice were treated with TMVP1-KLA peptide every 3 days for 28 days and then sacrificed. The tumors were surgically removed for LYVE1 staining. The frozen sections were fixed, then underwent rapid paraffin sectioning for immunohistochemistry of the corresponding blood vessels and lymphatic vessels and stained to reveal tumor changes and changes in the number of lymphatic vessels before and after treatment.

The experimental metastatic mouse model of 4T1 breast tumors was established as described above. The 150 μM TMVP1-KLA peptide or filter-sterile water was injected intraperitoneally every other day. Mice were sacrificed 21 days after the final therapy. The primary tumor weight and lung metastases were analyzed. The lung metastases were removed and fixed in 10% neutral-buffered formalin solution. These lung metastases were stained with H&E and safranin.

Statistical analysis

All *in vitro* experiments were repeated at least three times. The SPSS13.5 software package was used to analyze the data. Two-tailed Student's t-tests were used for comparisons between groups. A value of $P < 0.05$ was defined as statistically significant. All values were presented as the mean ± standard deviation (SD).

Results

Identification of a peptide that specifically binds to the extracellular domain of human VEGFR3.

We use the FliTrx™ Random Peptide Display Library, which is based on a random 12-mer cyclic peptide display library, to screen the binding peptides with recombinant human VEGFR-3/Flt-4.After four rounds, 100 individual FliTrx clones were selected and their peptide-encoding inserts were sequenced and analyzed for potential repetitive peptide motifs. Analyzing the core amino acids by computerized analysis, one of the peptide sequences enriched in the selected clone pool was RGLARGRIGFVM (Fig S1 A). To further confirm the affinity of the selected peptide with VEGFR-3, RGLARGRIGFVM was synthesized and the SPR assay was utilized to measure the binding affinity. As shown in Fig S1 B, the RGLARGRIGFVM exhibited the binding kinetics with a Kd value of 8.80×10^{-6} (M).

To further analyze which sequence represents the core binding sequence of RGLARGRIGFVM with VEGFR3, we sought to identify the amino acid residues of VEGFR-3 that could be involved directly in the peptide-protein interaction. To this end, the homology model of VEGFR-3 was built using Modeller software, and then a molecular docking simulation between RGLARGRIGFVM and VEGFR-3 was performed. The docking region sites revealed that D42, E136, F139, F215, and D212 (VEGFR-3 D1-2) are the amino acids near the binding pocket (Fig. S1 E). The LARGR on the polypeptide chain is well attached to the binding pocket, and the affinity and hydrophobic effects are well-matched, but the polypeptide amino acids on both sides of RGLARGRIGFVM cannot be combined with the binding pocket, but are free in aqueous solution (Fig. S1C and D). The interaction energy between protein and Peptide 1 (RGLARGRIGFVM) was -23.10 kcal/mol.

To validate the results of computational protein structure modeling, LARGR was synthesized, and the SPR assay and the docking method was also conducted. Fig. 1C, D, and E showed that LARGR docked in the same region of VEGFR-3 D1-2 as RGLARGRIGFVM, and LARGR exhibited significant binding with VEGFR-3. The Kd value (2.87×10^{-5} M) was similar to the 12-mer peptide (Fig. 1B), and the interaction energy was -16.77 kcal/mol.

FITC-TMVP1 binds with VEGFR-3 in vitro

The immunofluorescence ELISA assay showed that the binding of FITC-TMVP1 to recombinant Human VEGF R3/Flt4 protein was FITC-TMVP1 concentration-dependent. When 5 or 10 μg of FITC-TMVP1 was added, the immunofluorescence signal density was significantly increased compared to that of the control group (**, $P<0.01$) as shown in Fig. S 2B.

LECs, HUVEC, and HK293 cells were incubated with 20 μM FITC-labelled TMVP1 at 37℃ for 60 min, the affinity of FITC-TMVP1 to cells presented that the LECs had an optimal binding and internalization ability(Fig. 2B). For further clarification of the VEGFR-3 targeting ability of TMVP1, we constructed VEGFR-3-overexpressed cells using the lentiviral vector, western blotting, and immunofluorescent assay detected the expression of VEGFR-3, as shown in Fig S2C. VEGFR-3 was abundantly expressed in SiHa cells. VEGFR-3 over-expressed cells and control SiHa cells were incubated with 20 μM FITC-conjugated synthetic TMVP1 and VEGFR-3 antibody. Cell nuclei were stained with DAPI. The fluorescent images in the tumor cell were examined using laser confocal microscopy. The results showed that the location of

VEGFR-3 staining (red fluorescence) in the cell membrane was coincident with TMVP1 green fluorescence. Conversely, FITC-TMVP1 did not bind in the VEGFR-3-negative cells(Figure 2B).

FITC-TMVP1 targets lymphatic vessels in vitro and in vivo

To determine whether TMVP1 could target tumor lymphatic vessels in vivo, the corneal micropocket mouse 4T1 tumor model was established. As shown in Fig. 3A, 1 h after i.v. injection, the strong green fluorescence accumulated within the micro-bag cornea of tumor model, while only background fluorescence was observed in normal control Figure. At the same time, the tumor frozen sections were immunostained using VEGFR-3 antibody, the results showed that the VEGFR-3 staining (red fluorescence) in the vasculature was coincident with TMVP1 green fluorescence (Fig. 3B). The biodistribution of FITC-TMVP1 was mainly accumulated at the periphery of growing tumors (Fig. S3 A), in accordance with corneal micropocket mouse 4T1 tumor model, the VEGFR-3 staining (red fluorescence) in the vasculature was also coincident with TMVP1 green fluorescence in the 4T1 subcutaneous tumor model (Fig. S3 B).

The clinical tissue samples from breast cancer patients were dissected to study the binding specificity of TMVP1with neoplastic lymphatic vessels. A total of 12 human breast cancer specimens were analyzed in this study. The FITC-TMVP1 staining was observed to be completely coincident with anti-VEGFR-3, and partially colocalized with anti-LYVE1 staining with in all the 12 breast tumor sample (Fig. 3C).

TMVP1 targets tumor tissues as indicated by ^{99m}Tc labeling

The Kd value of HYNIC-TMVP1 with VEGFR-3 was 2.96×10^{-6} M. The SPR assay verified that the TMVP1 binding affinity with VEGFR-3 was not reduced (Fig 4B). Then HYNIC-TMVP1 was labeled with ^{99m}Tc, and the radiochemical purity of ^{99m}Tc-HYNIC/EDDA-TMVP1 was measured by radio-HPLC and ITLC-SG, the retention time was 13.48 min (Fig. S4 D), the radiochemical purity was greater than 95%. The solution stability of ^{99m}Tc-HYNIC/EDDA-TMVP1 was monitored by ITLC-SG in saline, in serum, and the presence of excess cysteine, and the radiotracer was stable in the all these solutions (Fig. S4 E).

Fig. 4C illustrates representative SPECT images of tumor-bearing mice at 30 min, 1 h, and 2 h after administration of ~ 18.5 MBq of ^{99m}Tc-labeled TMVP1 with or without excess TMVP1 pre-injection. The SPECT images showed that the B16 and 4T1 tumors were clearly visualized after administration, but SiHa tumors were poorly visualized. Meanwhile, the tumor imaging could be blocked by co-injection of excess cold TMVP1 (Fig. 4C and D). In addition, the radiotracer accumulated mainly in the kidney and bladder, which reflected the renal-mediated clearance of the radiotracer. IHC revealed VEGFR-3 expression in the above three tumor tissues. The results showed that the VEGFR-3 expression was in accordance with the accumulation of ^{99m}Tc-labeled TMVP1 (Fig. 4E).

To further understand the biodistribution characteristics of ^{99m}Tc-labeled TMVP1, nude mice bearing 4T1 xenografts were used to evaluate the biodistribution characteristics and excretion kinetics. Fig. S5A presents the %ID/g organ uptake for the tracer. In general, the radiotracer tumor uptake was 0.65 ± 0.09, and 0.314 ± 0.08 %ID/g at 2 h and 4 h, respectively, with extremely short blood retention times. The

tumor/blood ratios were 2.74 ±0.24 and 5.02 ±1.88 at 2 h and 4 h p.i., respectively (Fig. S5 B). The blocking experiment demonstrated that the accumulation of radiotracer could be significantly reduced by pre-injection of excess TMVP1 (Fig. S5 C).

TMVP1-KLA inhibits LECs to form lymphatic-like tube in vitro and in vivo. Three-dimensional visualization of *tube*-formation and the *in vitro* sprout forming assay were performed, and frank tube-like structures were observed in lymphatic endothelial cells, and their formation was enhanced by cytokine rhVEGF-C. When TMVP1-KLA or TMVP1-KLA plus rhVEGF-C were added, the numbers of lymphatic sprouts and tube-like structures were significantly reduced compared to the control groups, and some cells formed spherical apoptotic cells (Fig. 5A, B). The percentage of the average sprout length in TMVP1-KLA + rhVEGF-C- and TMVP1-KLA-treated LECs was, respectively, 5.2 ±1.1 % and 4.3+1.0 % significantly lower than that of rhVEGF-C-treated or control LECs. The percentage of tube-like structures coverage area in TMVP1-KLA + rhVEGF-C- and TMVP1-KLA-treated LECs were, respectively, 5.8 ±0.5 %, and 2.6 ± 0.4 %, which was significantly lower than that of the control.

To reveal the TMVP1-KLA inhibition of lymphangiogenesis, we chose the murine corneal transplantation model for our study. The number of lymphatic vessels found in the peptide-treated group was significantly less than that of the control group, as shown in Fig. 5C and D. Few lymphatic vessels were observed in the TMVP1-KLA treated group. The area of the LYVE1-positive staining in the TMVP1-KLA-treated group was 12.3 ±1.2 %, much less than that of the control group ($p<0.01$) (Fig. 5D). The arrangement of the tissue nuclei after TMVP1-KLA treatment was observed, with tightly packed nuclei and less lumen distribution. However, tissues in the control group were relatively loose, with more lumen structures.

TMTP1-KLA inhibits tumor lymphangiogenesis and development *in vivo.*

We next sought to explore whether the TMVP1-KLA peptide might represent a possible therapeutic strategy to suppress tumor lymphangiogenesis *in vivo.* We analyzed the effects of TMVP1-KLA on MDA-MB-231-derived orthotopic breast cancer lymphangiogenesis in mice. As shown in Fig. 6 A-C, TMVP1-KLA was observed to inhibit orthotopic breast tumor growth effectively. The mean tumor volumes of TMVP1-KLA-treated mice were 0.24 mm^3, which were significantly ($P < 0.05$) smaller than that of TMVP1-treated mice (0.87 ±0.07 mm^3; Fig. 6B). The tumor weight from the TMVP1-KLA group was 1.2 ±0.5 g, which was also significantly lower than that of the control group (Fig. 6C). Thus, TMVP1-KLA could significantly suppress tumor growth *in vivo* unlike TMTP1.

The tumor lymphangiogenesis vessel number of the mouse tumor tissue was observed between two groups using immunohistochemical staining. The area of LYVE1-positive staining decreased significantly in the TMTP1-KLA peptide-treated group compared to that in the control group (Figure 6D, E). Thus, these results showed a vigorous anti-lymphangiogenic effect of TMTP1-KLA peptide *in vivo.*

Effects of TMTP1-KLA on the inhibition of metastatic tumor cell extravasation into the lungs

An experimental lung metastasis model was applied to determine whether the TMTP1-KLA inhibition of metastasis was specifically due to decreased lymphatic vessels. In the TMVP1-KLA-treatment group, lung alveolar tissue and decreased numbers of cancer nests were observed, while in the control group, metastatic invasion left little alveolar lung tissue, as shown by HE staining. TMVP1-KLA effectively inhibited 4T1 subcutaneous tumor growth. The mean tumor volumes of TMVP1-KLA-treated mice were significantly ($P < 0.05$) smaller than those of control mice (as shown in Fig S6B). There were no deaths observed in mice treated with TMVP1-KLA.

Moreover, the lungs of TMVP1-KLA-treated mice showed significantly smaller volumes and fewer micro-metastases than that of control mice (Fig. S 6A, C; $P<0.01$). Histologically, TMVP1-KLA–treated mice showed clumps of metastatic cells lodged within lymphatic vessels that failed to breach the lymphatic basement membrane and enter the lung parenchyma (Fig. S 6A) (significantly more visible lung metastases were visualized in the control group; $P <0.01$). These experimental results showed that TMVP1-KLA could inhibit breast cancer growth and metastasis.

Discussion

Tumor lymphangiogenesis is required for lymph node metastasis. The targeting of VEGFR-3 will be therapeutically significant for human tumors[2, 12]. In line with this concept, we obtained a period of five TMVP1 peptide sequences using the extracellular domain of the recombinant active human protein VEGFR-3 by display random peptide library screening. Our combined immunofluorescence and autoradiography studies revealed that FITC-TMVP1 and ^{99m}Tc-labeled TMVP1 specifically accumulated in VEGFR-3-positive lymphatic vessels of tumors after i.v. administration in tumor xenograft *in vivo* models. The accumulation of TMVP1 in lymphatic vessels was specific, because which can be significantly reduced by blocking experiment. To investigate whether VEGFR3-targeted TMVP1 could be used to enhance the therapeutic efficacy of anticancer drugs, we synthesized a peptide conjugated with a proapoptotic peptide $_D$(KLAKLAK)^2. The fusion peptide strongly inhibited tumor lymphangiogenesis *in vitro* and *in vivo* and specifically suppressed lung metastasis in a 4T1 breast cancer xenograft model.

Small short peptides provide several possible advantages, including low immunogenicity, enhanced tissue penetration owing to their small size, ready diffusion, and ease of manufacture compared with larger biomolecules, such as antibodies. Previous studies describe the development of several kinds of VEGFR-3 targeting agents, including VEGFR-3 monoclonal antibodies, anticalins, peptides, and small pharmaceutical molecules[10, 11, 22, 23]. Tuulia Huhtala had shown that the 111In-labeled anti-VEGFR-3 antibody mF4-31C1 had a strong accumulation of the radioactivity in the tumor area, 48 h postinjection[24]. A typical feature of antibodies is their slow drug metabolism, unlike small pharmaceutical molecules and peptides *in vivo*. Li-Feng Shi screened a peptide with a sequence of WHWLPNLRHYAS targeting the extracellular fragment of recombinant human VEGFR-3/Flt-4 through a phage-displayed random peptide library, but the efficacy of binding affinity for homing targeting is not powerful[25]. Jen-Liang Sui identified two peptides which strongly inhibited the kinase activity of VEGFR-

3[26, 27]. Thus, the continued studies of VEGFR-3-targeting agents will be essential for developing new therapies that limit the spread of cancer.

In this work, we discovered TMVP1 binding with VEGFR3 by computerized analysis. One explanation for our results is this biopanning method was not an optimal strategy, And the Kd values of TMVP1 or the TMVP1 derivative tested in this study by SPR assays were about 10^{-6} magnitude, ^{99m}Tc-labeled TMVP1 underwent moderate tumor uptake (0.65 ± 0.09 and 0.314 ± 0.08% ID/g at 2 h and 4 h p.i., respectively) with extremely short blood retention times. The tumor/blood ratios were 2.74 ± 0.24 and 5.02 ± 1.88 at 2 h and 4 h p.i., respectively. To improve the binding affinity, stability, and biodistribution of TMVP1, several strategies including PEGylation, lipidation, and multimerization, have been employed. These modifications may decrease renal clearance, enhance water solubility, and improve delivery efficiency. Our future work will focus on the modifications of TMVP1 or the screening of novel peptides for VEGFR-3 binding.

Taken together, the TMVP1 peptide acquired using a random 12-mer cyclic peptide display library could specifically bind to LECs with high expression levels of VEGFR-3. The peptide TMVP1 with KLA can inhibit lymphangiogenesis *in vitro* and tumor growth and tumor intratumoral lymphatic vessels *in vivo*. The TMVP1 peptide would probably greatly improve the targeting efficiency of early tumor treatment if conjugated with anticancer drugs such as doxorubicin. It may also become a significant clinical tool for diagnostic and therapeutic repressors in targeting lymphangiogenesis and tumor metastasis, which thus will bring new opportunities and hope for the molecular therapy of tumors.

Declarations

Acknowledgements

None

Ethics approval and consent to participate

All animal experiments and tests were guided and approved by the Ethics Committee of Tongji Hospital, Tongji Medical College, Huazhong University of Science and Technology.(Approval No. TJH-201909010)

Consent for publication

All authors agree to be published

Availability of data and materials

All data generated or analyzed during this study are included in this published article.

Competing interests

Financial interests

The authors declare they have no financial interests.

Non-financial interests

None.

Founding

This work was supported by the grants from National Science Foundation of China (81802608, 81472444, 81472783, 81630060, 81601526) and the National Science-technology Supporting Plan Projects (2015BAI13B05) for their financial supports.

References

1. Golden, JA (2017). Deep Learning Algorithms for Detection of Lymph Node Metastases From Breast Cancer: Helping Artificial Intelligence Be Seen. Jama **318**: 2184–2186.
2. Tammela, T, and Alitalo, K (2010). Lymphangiogenesis: Molecular mechanisms and future promise. Cell **140**: 460–476.
3. Wuthrick, EJ, and Harrison, LB (2019). A Deep Dive into the Diagnosis and Management of Regional Lymph Node Metastases. Seminars in radiation oncology **29**: 91–92.
4. Leppanen, VM, Tvorogov, D, Kisko, K, Prota, AE, Jeltsch, M, Anisimov, A, *et al.* (2013). Structural and mechanistic insights into VEGF receptor 3 ligand binding and activation. Proceedings of the National Academy of Sciences of the United States of America **110**: 12960–12965.
5. Baker, E, Whiteoak, N, Hall, L, France, J, Wilson, D, and Bhaskar, P (2019). Mammaglobin-A, VEGFR3, and Ki67 in Human Breast Cancer Pathology and Five Year Survival. Breast cancer: basic and clinical research **13**: 1178223419858957.
6. Crona, DJ, Skol, AD, Leppanen, VM, Glubb, DM, Etheridge, AS, Hilliard, E, *et al.* (2019). Genetic Variants of VEGFA and FLT4 Are Determinants of Survival in Renal Cell Carcinoma Patients Treated with Sorafenib. Cancer research **79**: 231–241.
7. Sallinen, H, Anttila, M, Narvainen, J, Koponen, J, Hamalainen, K, Kholova, I, *et al.* (2009). Antiangiogenic gene therapy with soluble VEGFR-1, -2, and – 3 reduces the growth of solid human ovarian carcinoma in mice. Molecular therapy: the journal of the American Society of Gene Therapy **17**: 278–284.
8. Martinez-Corral, I, Stanczuk, L, Frye, M, Ulvmar, MH, Dieguez-Hurtado, R, Olmeda, D, *et al.* (2016). Vegfr3-CreER (T2) mouse, a new genetic tool for targeting the lymphatic system. Angiogenesis **19**: 433–445.
9. McDonald, DM (2010). New antibody to stop tumor angiogenesis and lymphatic spread by blocking receptor partnering. Cancer cell **18**: 541–543.
10. Richter, A, and Skerra, A (2017). Anticalins directed against vascular endothelial growth factor receptor 3 (VEGFR-3) with picomolar affinities show potential for medical therapy and in vivo

imaging. Biological chemistry **398**: 39–55.

11. Roberts, N, Kloos, B, Cassella, M, Podgrabinska, S, Persaud, K, Wu, Y, *et al.* (2006). Inhibition of VEGFR-3 activation with the antagonistic antibody more potently suppresses lymph node and distant metastases than inactivation of VEGFR-2. Cancer research **66**: 2650–2657.
12. Hsu, MC, Pan, MR, and Hung, WC (2019). Two Birds, One Stone: Double Hits on Tumor Growth and Lymphangiogenesis by Targeting Vascular Endothelial Growth Factor Receptor 3. *Cells* **8**.
13. Teesalu, T, Sugahara, KN, and Ruoslahti, E (2013). Tumor-penetrating peptides. Frontiers in oncology **3**: 216.
14. Sioud, M (2019). Phage Display Libraries: From Binders to Targeted Drug Delivery and Human Therapeutics. Molecular biotechnology **61**: 286–303.
15. Fosgerau, K, and Hoffmann, T (2015). Peptide therapeutics: current status and future directions. Drug discovery today **20**: 122–128.
16. Mai, JC, Mi, Z, Kim, SH, Ng, B, and Robbins, PD (2001). A proapoptotic peptide for the treatment of solid tumors. Cancer research **61**: 7709–7712.
17. Ma, X, Xi, L, Luo, D, Liu, R, Li, S, Liu, Y, *et al.* (2012). Anti-tumor effects of the peptide TMTP1-GG-D(KLAKLAK)(2) on highly metastatic cancers. PloS one **7**: e42685.
18. Fung, S, and Hruby, VJ (2005). Design of cyclic and other templates for potent and selective peptide alpha-MSH analogues. Current opinion in chemical biology **9**: 352–358.
19. Li, F, Cheng, T, Dong, Q, Wei, R, Zhang, Z, Luo, D, *et al.* (2015). Evaluation of (99m)Tc-HYNIC-TMTP1 as a tumor-homing imaging agent targeting metastasis with SPECT. Nuclear medicine and biology **42**: 256–262.
20. Li, F, Zhang, Z, Cheng, T, Wei, R, Dai, Y, Lv, M, *et al.* (2016). SPECT imaging of interleukin-6 receptor in ovarian tumor xenografts with a novel radiotracer of 99mTc-HYNIC-Aca-LSLITRL. Amino acids **48**: 91–101.
21. Rogers, MS, Birsner, AE, and D'Amato, RJ (2007). The mouse cornea micropocket angiogenesis assay. Nature protocols **2**: 2545–2550.
22. Tammela, T, Zarkada, G, Wallgard, E, Murtomaki, A, Suchting, S, Wirzenius, M, *et al.* (2008). Blocking VEGFR-3 suppresses angiogenic sprouting and vascular network formation. Nature **454**: 656–660.
23. Urner, S, Planas-Paz, L, Hilger, LS, Henning, C, Branopolski, A, Kelly-Goss, M, *et al.* (2019). Identification of ILK as a critical regulator of VEGFR3 signalling and lymphatic vascular growth. The EMBO journal **38**.
24. Huhtala, T, Laakkonen, P, Sallinen, H, Yla-Herttuala, S, and Narvanen, A (2010). In vivo SPECT/CT imaging of human orthotopic ovarian carcinoma xenografts with 111In-labeled monoclonal antibodies. Nuclear medicine and biology **37**: 957–964.
25. Shi, LF, Wu, Y, and Li, CY (2015). Identification of high-affinity VEGFR3-binding peptides through a phage-displayed random peptide library. Journal of gynecologic oncology **26**: 327–335.

26. Chang, YW, Su, CM, Su, YH, Ho, YS, Lai, HH, Chen, HA, *et al.* (2014). Novel peptides suppress VEGFR-3 activity and antagonize VEGFR-3-mediated oncogenic effects. Oncotarget **5**: 3823–3835.
27. Wu, D, Tian, W, Li, J, Zhang, Q, Wang, H, Zhang, L, *et al.* (2019). Peptide P11 suppresses the growth of human thyroid carcinoma by inhibiting the PI3K/AKT/mTOR signaling pathway. Molecular biology reports **46**: 2665–2678.

Figures

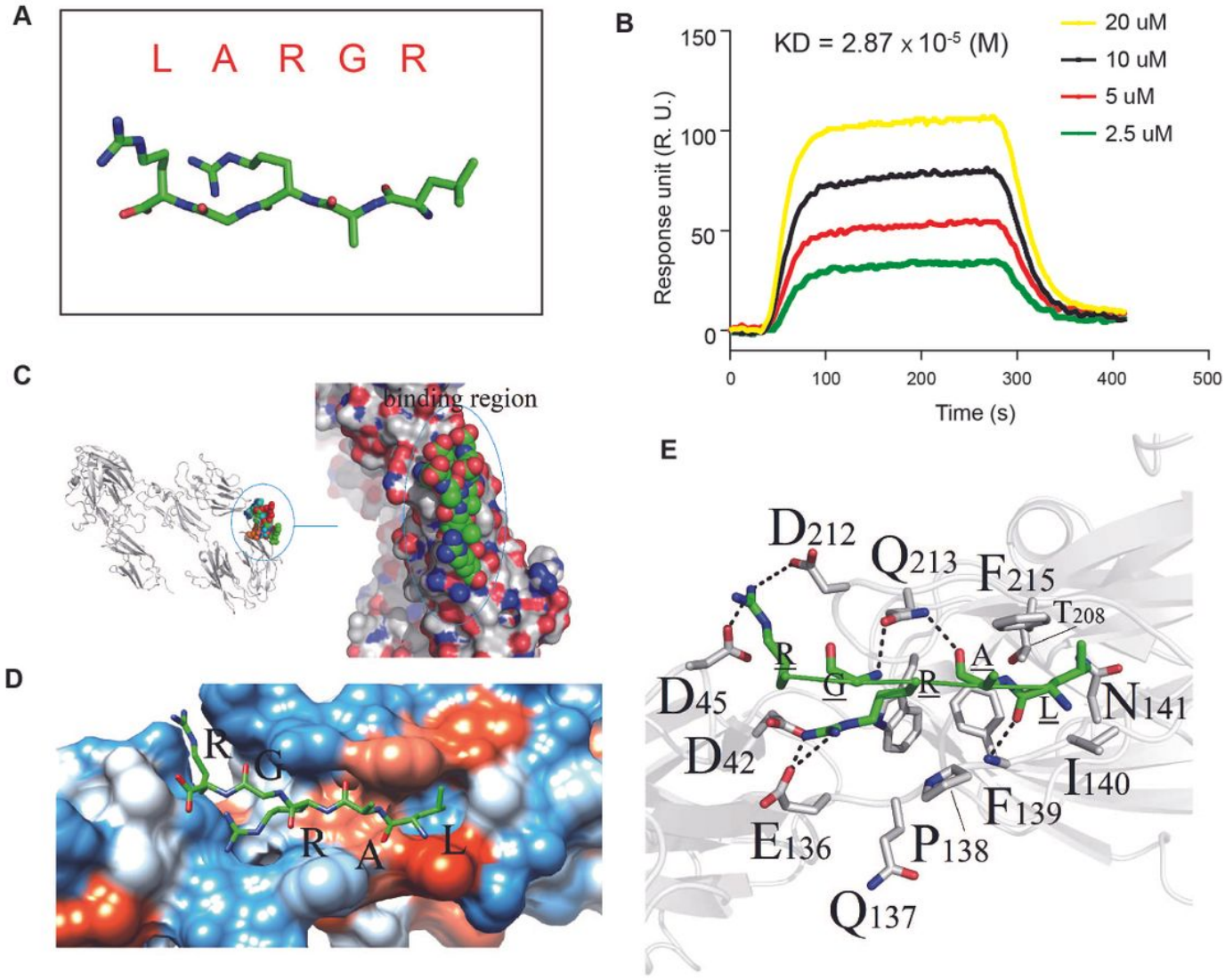

Figure 1

The structure of TMVP1 and its affinity and specificity to VEGFR-3 protein. A. The amino acid sequence (upper) and structure (lower) of TMVP1. B. The OpenSPR™ assay determined the binding kinetics constants (Kd) between TMVP1 and the human recombinant VEGFR-3 proteins. C. The homology model of VEGFR-3 was built using Modeller software, then molecular docking simulation between LARGR and VEGFR-3 were performed, and the general view of the binding region of TMVP1 with VEGFR-3 is shown.

D. The surface cartoon view of the VEGFR-3 hydrophobic pocket occupied by the docked poses for LARGR. E. The closer view of the amino acids in the binding site for VEGFR-3 with TMVP1.

Figure 2

In vitro specific binding of FITC-TMVP1 in VEGFR-3-overexpressing cells. A. The cell lines hLEC, HUVEC, and HK293 weretreated with FITC-TMVP1 and immunostained by VEGFR-3 antibody, and the fluorescent images was obtained. B. FITC-TMVP1 was incubated with SiHa-con) and SiHa-VEGFR-3(B) cells, and the VEGFR-3 expression was simultaneously detected using immunofluorescence microscopy.

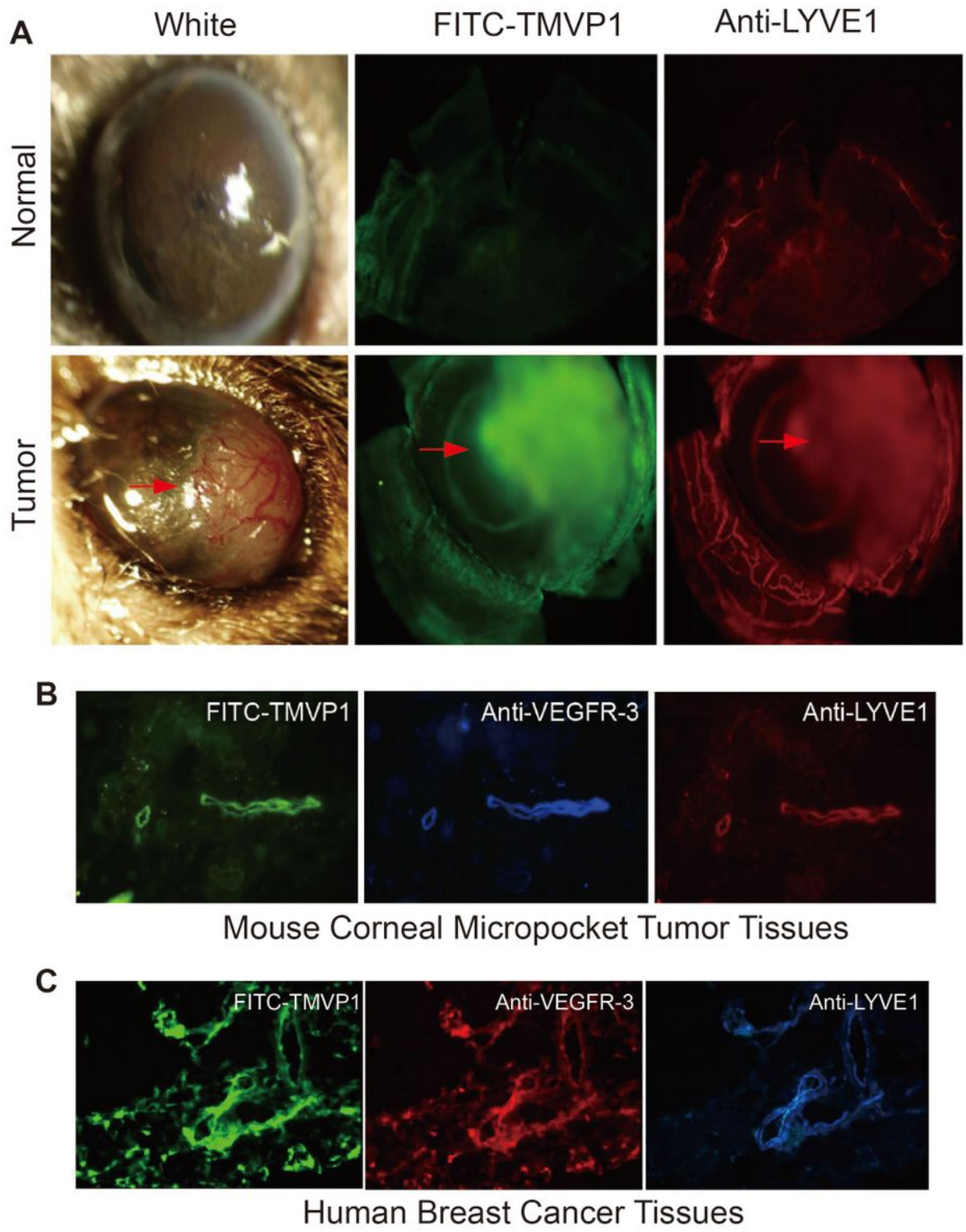

Figure 3

FITC-TMVP1 peptide is co-localized with lymphatic vessel markers in vivo. A. The mouse corneal micropocket tumor model was established, then FITC-TMVP1 was injected into the mouse by the tail vein. Representative images of white and green fluorescence were obtained using a slit-lamp biomicroscope (the red arrow indicates the location of tumors). B. The tumor tissues were excised and stained with anti-LYVE1 (red) and anti-VEGFR-3 (blue); representative images from confocal laser scanning microscopy are

shown. C. The tumor lymphatic targeting capacity of TMVP1 was measured in breast cancer tissues. TMVP1 was coincident with anti-VEGFR-3 and anti-LYVE1 staining in the same field.

Figure 4

The tumor targeting of TMVP1 as indicated by SPECT imaging of 99mTc-HYNIC/EDDA-TMVP1 in a xenograft tumor model. A. The TMVP1 peptide was labeled with 99mTc, and the structure of 99mTc-HYNIC/EDDA-TMVP1 is shown. B. The SPR assay determined the affinity of 99mTc-HYNIC/EDDA-TMVP1 for VEGFR-3. C. Representative coronal SPECT images of mice bearing B16 (upper), 4T1 (middle), and SiHa tumors (lower) at 30, 60, and 120 min after 99mTc-HYNIC/EDDA-TMVP1 administration. D. The ratios of radioactivity counts in the tumor to the contralateral side were measured. E. Meanwhile, the expression of VEGFR-3 was detected using IHC.

Figure 5

TMVP1 peptide reduces lymphatic sprouting and lymphangiogenesis by conjugating a proapoptotic peptide D(KLAKLAK)2 in vitro and in vivo. A. LECs were pretreated with rhVEGF-C or TMVP1-KLA for 24 h. Capillary-like tube formation was observed, and photographs were captured at 6 h and 16 h after incubation. B. Sprouting and capillary-like tube lengths were quantified. C. TMVP1-KLA-treated mice in the traditional corneal assay showed significantly decreased lymphangiogenesis in the cornea compared with controls. Representative images of white and LYVE1 staining by immunohistochemistry and microscopy showing significantly reduced lymphatic vessels in mouse corneas after TMVP1-KLA treatment. D. Quantification of LYVE-1-positive signals from 5–6 optical fields in different sections.

Figure 6

TMVP1-KLA inhibited the lymphatic angiogenesis of nude mice bearing MDA-MB-231-derived human breast carcinoma xenografts. A. Mice bearing MDA-MB-231 breast carcinoma cells treated with TMVP1-KLA peptide were smaller than those treated with control peptide. B. Tumor volumes of mice treated with TMVP1-KLA peptide or not were measured. C. Tumor weights were assessed on day 40. P 0.05, using Student's t-test. D. Analysis of lymphatic vessel density in tumor samples using an immunohistochemistry assay. The lymphatic vessel density decreased notably in TMVP1-KLA peptide–treated tumors. E. The quantification of LYVE-1-positive signals from 5–6 optical fields of different sections.

Supplementary Files

This is a list of supplementary files associated with this preprint. Click to download.

- SupplementFigure101.jpg
- supplementFigure2101.jpg
- supplementFigure3.jpg
- SupplementFigure401.jpg
- supplementFigure501.jpg
- supplementFigure6.tif
- SupplementFigure7.tif